



Published in final edited form as:

ACS Catal. 2018 May 4; 8(5): 3754–3763. doi:10.1021/acscatal.8b00105.

Iridium Catalysts for Acceptorless Dehydrogenation of Alcohols to Carboxylic Acids: Scope and Mechanism

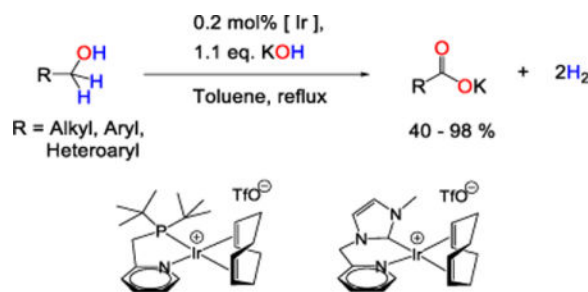
Valeriy Cherepakhin and Travis J. Williams*

Donald P. and Katherine B. Loker Hydrocarbon Institute and Department of Chemistry, University of Southern California, Los Angeles, California, 90089-1661, United States

Abstract

We introduce iridium-based conditions for the conversion of primary alcohols to potassium carboxylates (or carboxylic acids) in the presence of potassium hydroxide and either [Ir(2-PyCH₂(C₄H₅N₂))(COD)]OTf (**1**) or [Ir(2-PyCH₂P^tBu₂)¹(COD)]OTf (**2**). The method provides both aliphatic and benzylic carboxylates in high yield and with outstanding functional group tolerance. We illustrate the application of this method to a diverse variety of primary alcohols, including those involving heterocycles and even free amines. Complex **2** reacts with alcohols to form crystallographically-characterized catalytic intermediates [IrH(η^1, η^3 -C₈H₁₂)(2-PyCH₂P^tBu₂)] (**2a**) and [Ir₂H₃(CO)(2-PyCH₂P^tBu₂) $\{\mu$ -(C₅H₃N)CH₂P^tBu₂}] (**2c**). The unexpected similarities in reactivities of **1** and **2** in this reaction, along with synthetic studies on several of our iridium intermediates, enable us to form a general proposal of the mechanisms of catalyst activation that govern the disparate reactivities of **1** and **2**, respectively in glycerol and formic acid dehydrogenation. Moreover, careful analysis of the organic intermediates in the oxidation sequence enable new insights into the role of Tishchenko and Cannizzaro reactions in the overall oxidation.

TOC image



*Corresponding Author: TJW: travisw@usc.edu.

Supporting Information

The Supporting Information is available free of charge on the ACS Publications website at DOI: 10.1021/**.

Experimental procedures, graphical and tabular characterization information (PDF)

Notes

The authors declare no competing financial interests.

Keywords

Acceptorless dehydrogenation; Iridium; Metal hydride; Alcohol; Carboxylic acid

INTRODUCTION

Oxidation of primary alcohols to carboxylic acids is a quintessential transformation in organic chemistry, historically accomplished with a stoichiometric portion of a metal-based oxidant, such as potassium permanganate,^{1,2} chromium(VI) oxide,³ pyridinium dichromate,⁴ RuCl₃/NaIO₄,⁵ sodium hypochlorite,⁶ or the like. These evolved, ultimately to culminate in Lindgren (and related) oxidation of aldehydes, the mild conditions of choice for complex molecule synthesis. Still, some forcing conditions to dehydrogenate primary alcohols directly to carboxylates have been known since the 19th century. For example, J. B. Dumas (1840) and later E. Reid et al.⁷ converted primary alcohols to carboxylate salts and H₂ by heating with hydroxide at 350 °C. This approach has recently advanced to emerge as an elegant 21st-century replacement for the stoichiometric oxidant methods, which is important, because alcohol to carboxylate conversion remains a frequent operation in complex molecule synthesis.^{8–11}

Carboxylate synthesis by acceptorless dehydrogenation presents a graceful approach with the recent development of new catalytic conditions, some enabling the reaction under very convenient conditions (25 – 120 °C, 1 atm). To date, homogeneous catalysts for this reaction include systems based on rhodium, ruthenium, and recently one iridium complex. The former include a diolefin amido tridentate ligand and catalyze hydrogen transfer from alcohols to acceptors like cyclohexanone,¹² 1-hexene,¹³ or O₂/DMSO.¹⁴ Ruthenium complexes featuring tridentate PNN,¹⁵ PNP,¹⁶ and NHC-ligands,¹⁷ catalyze acceptorless dehydrogenation. The Cp*Ir^{III} system enables reactions in neutral water.^{17a} The former reactions take place in boiling NaOH solutions and give high yields of aliphatic carboxylates and benzoates. Such reactions also are possible in refluxing toluene¹⁸ and neat alcohol (150 °C).¹⁹

We recently reported very robust catalysts for acceptorless dehydrogenation of formic acid (based on **2**, Figure 1)²⁰ and glycerol (**1**, **4**),²¹ with the latter giving an example of excellent selectivity for primary alcohol oxidation in the presence of other molecular complexity. In this study we report that these same iridium-based systems enable a method for acceptorless dehydrogenation of primary alcohols to carboxylic acids. This method gives good yields of many carboxylates and enables selectivity that is difficult to achieve with other catalytic systems. We show broad substrate scope, including reactions of alcohols with a secondary amino group or aryl halide, and report unanticipated features of the catalytic mechanism. Particularly, we show details of catalyst initiation and provide a unifying proposal of the mechanisms of catalyst activation that govern the disparate reactivities of **1** and **2**, respectively in glycerol and formic acid dehydrogenation.

RESULTS AND DISCUSSION

Alcohol Oxidation

The discovery and optimization of our reaction is outlined in Table 1. The material balance of the reaction involves one equivalent of hydroxide. However, any base in the reaction will cause a parallel Guerbet self-condensation.⁷ For example,²² neat 1-octanol (**6b**) converts to potassium octanoate (**7b**, 72%) and 2-octyl-1-octanol (**8b**, 28%) in the presence of 1 eq. of potassium hydroxide and **1** (1 mol%) at 150 °C (yields calculated by NMR). In order to suppress this side-reaction, we conduct the dehydrogenation in a solvent of refluxing toluene: here, 1-octanol gives 99% of octanoate, 1% of Guerbet alcohol **8b** after 40 h. This solvent choice contrasts many examples of primary alcohol dehydrogenation in the literature,^{15–17} in which reactions are typically run in water. Complex **1** is less effective in an aqueous medium, and the yield of octanoate is only 7% after 40 h. The origin of selectivity for carboxylate formation appears to be solubility: hydroxide's limited solubility in toluene limits the total base concentration available for the Guerbet side reaction. In our hands, toluene is useful for most alcohols; diols and triols have limited solubility, and thus limited reactivity.

Table 1 shows the performance of our iridium pre-catalysts in alcohol dehydrogenation in toluene. The most effective catalyst, typically **1** or **2** in different cases, was determined among our available iridium(I) complexes (Figure 1) on the basis of product yield and selectivity. 1-Butanol (**6a**), 1-octanol (**6b**), and 1-hexadecanol (**6c**) were used as substrates. The selectivity for carboxylate synthesis decreases with increased molecular weight of the alcohol, which we believe to be an effect of base solubility.

Relative rates of catalysis for complexes **1**, **2**, and **5** were evaluated by recording hydrogen evolution in the conversion of benzyl alcohol (**6f**) to benzoate. Benzyl alcohol was chosen to avoid a Guerbet reaction. Kinetic profiles of hydrogen evolution demonstrate that complex **2** has the highest catalytic activity (Figure 2). Though **2** proved to be the fastest catalyst among the iridium compounds, complex **1** was also examined in substrate scope studies.

Application of the optimized reaction conditions enabled an effective conversion of a variety of primary alcohols to potassium carboxylates (Table 2). Substrate scope includes aliphatic alcohols (entries 1 – 5), benzylic alcohols (entries 6 – 12), and even heteroatom functionalized systems like thioethers (entry 8), amino alcohols (entries 13 and 14) and heterocycles (entries 16 and 17). This latter class of substrates is unknown for other catalytic systems for this reaction, including the one based on iridium.

Several generalizations can be drawn from these data. Unfunctionalized alkyl systems proceed smoothly (entries 1-3), and an adjacent strained ring is not derivatized in the reaction (entry 4). Sterically bulky systems can be problematic. For example, entries 5 and 18 demonstrate that a 1-adamantyl substituent (**6e**) slows the reaction, ca. half the rate, although it reaches completion. A doubly-blocked 2,6-dimethylbenzyl alcohol (**6r**) is unreactive.

Although aryl bromides and iodides are only moderately tolerated, entries 10 and 11 give examples of Ar-Br and Ar-I bonds surviving alcohol dehydrogenation conditions. We observe reduction (to Ar-H groups) as the major side reaction in these cases.¹⁸ For example, 4-bromobenzyl alcohol (**6j**) undergoes dehydrogenation to form both the corresponding 4-bromobenzoate (58%) and the reduced benzoate (9%) product. 4-Iodobenzyl alcohol (**6k**) afforded a larger amount of dehalogenated benzoate (32%) in addition to the halogenated product (42%). In contrast to aryl bromides and iodides, aryl chlorides are well tolerated (entry 9), and afford access to a growing number of metal-catalyzed coupling reactions.²³

Secondary amines and azoles are tolerated. Whereas several iridium complexes catalyze alkylation of primary amines with alcohols,^{24,25} we were curious how an amino alcohol would fare in our conditions. We found that we can convert amino alcohol **6m** efficiently to the corresponding amino acid without polymerization or other side reactions. This presents an unprecedented approach to amino acid synthesis. We further find that intramolecular oxidative cyclization of amino alcohols is possible: dehydrogenation of **6n** results in cyclization, yielding indole **7n** exclusively.^{24a}

We observe good selectivity for carboxylate synthesis in cases where arene hydrogenation or reductive decarboxylation can take place. For example, alcohol **6l** gives a high yield (84%, entry 12) of the corresponding carboxylic acid, however, we also observe trace quantities of naphthalene, 1,2-dihydronaphthalene, tetralin, and potassium formate in the reaction mixture. Quinoline **6q** is even more susceptible to over-reduction, yet we see only a trace of the corresponding tetrahydroquinoline in the crude product mixture of **7q**. By contrast, an attempt to dehydrogenate 2-(hydroxymethyl)thiophene and 3-phenylpropargyl alcohol resulted in product decarboxylation, giving potassium formate. Unfortunately, alkenes and nitro compounds are incompatible with our conditions and undergo uncontrolled reduction.

We showed that our catalytic systems can be applied to large-scale synthesis of carboxylic acids. Complexes **1** and **2** convert benzyl alcohol to benzoic acid with turnover numbers 16400 and 40600 respectively. Pre-catalyst **2** loading can be as low as 50 ppm to give up to 15 g of benzoic acid. Moreover, precipitation of the carboxylate during the reaction enables easy separation of the product by simple filtration. The catalyst-containing toluene solution can then be reused.

The catalytic method presented here is the second example we know for iridium based primary alcohol dehydrogenation. The previously reported method by Fujita utilizes Ir^{III} pre-catalyst [Cp*Ir(NC)(H₂O)](OTf)₂ (NC – pyridylcarbene bidentate ligand).^{17a} An advantage of the method is the possibility to conduct alcohol oxidation under base-free conditions, whereas our method requires stoichiometric KOH. Fujita's method uses high catalyst loading (2 – 5 mol%) and the reaction scope is confined to simple benzyl alcohols, with reactions of aliphatic alcohols giving yields of <25%. Thus, our method is a useful complement to the Fujita's chemistry.

Mechanism

The near-interchangeability of **1** and **2** in the conversions of **6** to **7** was not anticipated. We observe very different reactivity of these species respectively in glycerol²¹ and formic acid²⁰

dehydrogenation: **1** works only in the former and **2** only in the latter. Carboxylate synthesis thus provides us with a platform from which to run comparative stoichiometric reactions of **1** and **2** (Scheme 1) to gain insight into both the mechanisms of catalyst initiation and the differences in their reactivities.

Complex **1** reacts with neat alcohol **6g** in the presence of potassium hydroxide to form iridium(I) alkoxide complex **1a**, which can be extracted from potassium salts with C₆D₆. The structure of **1a** was established by NMR, with the coordination geometry assigned by NOE analysis (see Supporting Information). The complex retains its bidentate N—C ligand without proton loss, and the aryl alkoxide ligand exchanges slowly ($k \sim 1 \text{ s}^{-1}$) with excess **6g** in solution. Complex **1a** is reactive in benzene solution in the presence of excess **6g**, converting it to 4-methoxybenzyl-4-methoxybenzoate (**1b**). The iridium-containing species precipitates from solution leaving cyclooctene. These data are consistent with hydrogen transfer from **6g** to coordinated 1,5-cyclooctadiene to give reduction of one its olefins. We observe the same of **1** in glycerol dehydrogenation.²¹ Importantly, we see no evidence of an iridium hydride or any other metallic intermediate in this sequence.

Complex **2** reacts with **6g** or isopropanol to give iridium(III) complex **2b** (Scheme 1), which can be isolated in 64% yield. The structure of **2b** was established by single-crystal X-ray diffraction (Figure 3). It is analogous to the structure of [IrH(η^1, η^3 -C₈H₁₂)(dppm)], reported by Werner and co-workers.²⁶ We believe that an intermediate iridium alkoxide is involved in the formation of **2b**, but unlike **1a**, this converts to a stable iridium hydride species. We believe that this is the same initiation sequence observed for **2** in the dehydrogenation of formic acid, because **2b** is easily converted to **2d**, a form of the active catalyst of formic acid dehydrogenation initiating from **2**.²⁰

Complex **2** reacts with 1-butanol and potassium hydroxide in boiling toluene to form dinuclear iridium(II) complex **2c** (Scheme 1), which is isolated in 63% yield. Its structure, shown in Figure 3, has two notable features: a single CO ligand and a bridging *ortho*-metalated pyridine fragment. The CO ligand derives from *n*-butanal,^{27–30} and several cases of pyridine *ortho*-metalation by iridium complexes have been described.^{31–33} ¹H NMR of **2c** shows three hydride ligands; their arrangement in the coordination sphere was confirmed by COSY, NOESY/EXSY, and ¹H – ³¹P HMBC experiments (see Supporting Information).

Complex **2c** is stable in the solid state and in solution at room temperature in the absence of air, however it undergoes reversible isomerization to **2f** in toluene at 110 °C (Scheme 2). According to ¹H NMR data, heating the solution of pure **2c** leads to disappearance of the two *cis*-hydride signals and reduction of types of *tert*-butyl groups from four to two. This indicates that **2c** is involved in a fast dynamic equilibrium with a symmetrical species, which we propose to be the product of Ir–H–Ir bridge cleavage **2e**. The next step is slow, and the system comes to equilibrium only after four hours ($K_{\text{eq}} = [\mathbf{2f}]/[\mathbf{2c}] = 0.626$; $\Delta G_{383}^\circ = 360 \text{ cal/mol}$; $k_1 = 1.4(1) \times 10^{-4} \text{ s}^{-1}$; and $k_{-1} = 2.2(1) \times 10^{-4} \text{ s}^{-1}$). The equilibrated mixture at room temperature contains chemical shifts of pure **2c** and **2f** only.

The structure of **2f** was established by NMR studies. ¹H spectrum contains two hydride peaks in the ratio 1 : 2 at –6.64 (d, ²J_{PH} = 150.4) and –8.98 (br. s) ppm respectively. Seven

aromatic peaks indicate that **2f** has two ligands and one of them is *ortho*-metalated. Two doublets of the four *tert*-butyl groups indicate the presence of a symmetry plane in the molecule. $^1\text{H} - ^{31}\text{P}$ HMBC experiment demonstrates coupling between different hydrides (-6.64 , and -8.98 ppm) and different phosphorus nuclei (63.79 , and 88.66 ppm respectively). Hence, the only reasonable molecular structure must have all three hydrides bound to one iridium center. We assign this structure as **2f** in scheme 2.

Complex **2c** reacts with 10 eq. of *n*-hexanal at room temperature. This initially produces a number of unidentified iridium hydride complexes. After two days at $80\text{ }^\circ\text{C}$ the reaction reaches completion and all the transient iridium hydrides turn to a single complex, **2g** (Scheme 2). Its structure was determined with NMR and MALDI-MS data. The ^1H NMR spectrum of **2g** contains two peaks of the hydride ligands at -8.44 (ddd) and -11.15 (ddd) ppm and six aromatic peaks, suggesting that both pyridine fragments are *ortho*-metalated. No chemical exchange (EXSY) was observed between the hydride ligands, which is consistent with their proposed *trans* configuration. Complex **2g** has two hydrogen atoms fewer than **2c**, meaning that it is a dehydrogenated form of **2c**. The identified organic products in this reaction are 1-hexanol and hexyl hexanoate. 1-Hexanol is the product of hydrogen transfer from **2c** to *n*-hexanal, and hexyl hexanoate is the product of Tishchenko dimerization. Hexanal remains present in the mixture after prolonged heating, showing that **2g** does not catalyze its disproportionation; this is most likely accessed via one of the transient iridium hydrides mentioned above. Reduction of **2g** back to **2c** by 1-hexanol or H_2 (1 atm) at $110\text{ }^\circ\text{C}$ in toluene is not detected, even after 12 h.

When **2** reacts with 1-butanol and KOH in boiling toluene a mixture of iridium hydride complexes is formed, in which **2c**, **2f**, and **2g** are the major components (Figure 4). Moreover, we showed that **2c** is active in benzyl alcohol dehydrogenation with an identical kinetic profile to **2**. These facts suggest that **2c**, **2f**, and **2g** are the catalyst resting states which convert among each other during alcohol dehydrogenation with pre-catalyst **2**.

Whereas the interconversion of **2c** and **2f** is accessed at elevated temperature, it is unclear how **2c** can convert reversibly to **2g** in the catalytic process. Nevertheless, we showed this transformation to be involved in the catalytic mechanism by conducting deuteration experiment. Treatment of **2c** with 1-hexanol- $O,1,1-d_3$ (**6s**) under dehydrogenation conditions (Scheme 2) reveals partial deuteration of all three hydrides and the pyridine *ortho*-hydrogen in equal portions. Thus, all three hydrides are reversibly derivatized under the catalytic conditions. Since **2g** contains two *ortho*-metalated pyridine fragments we propose it as the intermediate in the *ortho*-deuteration of the free pyridine fragment of **2c**.

The linking methylene group of complex **2c** has an acidity comparable to that of alcohols (Scheme 2), but we do not observe the deprotonated form as a major species in catalysis. For example, we observe that treating yellow solution of **2c** with *t*-BuOK in benzene gives red-colored complex **2h** (Scheme 2). A ^1H NMR spectrum of **2h** shows selective deprotonation of benzylic arm of the metalated ligand and dearomatization of the corresponding pyridine system. The hydride ligands remain intact. Similar reactivity of structurally related PNP pincer ligands with similar colorimetric behavior was reported by Milstein.³⁴ Complex **2h**

undergoes complete protonation by 1-hexanol to return initial **2c**, indicating that **2c** is more acidic than *t*-BuOH, but less acidic than 1-hexanol.

Scheme 3 illustrates the proposed mechanism of catalyst generation and catalytic alcohol dehydrogenation using complex **2** as a pre-catalyst. We believe that both **1** and **2** initiate through analogous sequences, but that the hydrides of **1** are high energy, and are thus not observed. We believe that the difference in hydride stabilities is a consequence of the subtle electronic differences between the respective carbene and phosphine groups of **1** and **2**. The first step involves a nucleophilic attack of an alkoxide anion on **2**, producing iridium(I) alkoxide **2a**, which is the structural analogue of **1a**. Species **2a** undergoes β -hydride elimination to give an aldehyde and complex **2b**, the mechanism of this transformation had been studied previously on a similar iridium complex.²⁶

Complex **2b** is stable at room temperature, and subsequent intermediates were accessed at elevated temperature. We find that **2b** forms complex mixtures of iridium hydride species when reacted with 1-butanol or *n*-hexanal at 80 °C, however, complex **2c** was detected after reaction with *n*-hexanal. Hence, we conclude that **2b** can be converted to **2c** by an aldehyde produced in the conversion of **2a**. This gives our system access to the **2c/2f** equilibrium. Since we have shown that **2c** reacts with *n*-hexanal rather than 1-hexanol, we believe that the next step of the mechanism involves reversible reaction between **2e** and an aldehyde, ultimately leading to **2g**. We suggest that one of the intermediates in this reaction is the jumping-off point for the catalytic process (“Active Catalyst”, scheme 3). We expect the catalytic cycle to proceed by a traditional β -hydride elimination from an intermediate iridium alkoxide. We expect this to be irreversible, because toluene solutions of **2c**, **2f**, and **2g** do not react with H₂ (1 atm) at either 25 or 110 °C. Although we could not fully characterize the chain of all iridium species involved, all of them that we have are dinuclear, starting from **2c**.

Our studies on the organic intermediates involved in the alcohol dehydrogenation process turned up two unexpected observations (Scheme 4). First, formation of ester by-products rules in the possibility of Tishchenko like reaction of an intermediate aldehyde. Second, kinetic evidence necessitates Cannizzaro reaction in the mechanism of oxidation of benzyl alcohols.

Synthesis of **1a** is illustrated in scheme 1. We find that upon exposure to our catalytic conditions at 25 °C, this material generates 4,4'-dimethoxybenzyl benzoate, which indicates that Tishchenko like reaction of 4-methoxybenzaldehyde is faster than its direct conversion to **7g**. Moreover, formation of hexyl hexanoate in the reaction between **2c** and *n*-hexanal shows that ester generation is also possible when pre-catalyst **2** is used. In order to verify our proposed Tishchenko pathway, we showed that a significant portion of an aldehyde exists in the hemiacetal form under catalytic conditions: NMR data show that *n*-hexanal reacts with an excess of 1-butanol in the presence of catalytic KOH in toluene to give the corresponding hemiacetal (1-butoxyhexan-1-ol). Thus, we must consider ester formation as a route in the mechanism of carboxylate synthesis (Scheme 4A).

Aromatic aldehydes undergo Cannizzaro reaction in the presence of KOH to give the corresponding benzyl alcohols and carboxylates (Scheme 4B). Such disproportionation is known under our conditions in the absence of iridium (1 h, KOH, toluene, 110 °C).¹⁸ In our conditions, the resulting alcohol converts to aldehyde via iridium catalyzed dehydrogenation. We are convinced that Cannizzaro reaction must be happening, because when benzaldehyde is used instead of an alcohol under typical dehydrogenation conditions, it takes ca. 30 min for hydrogen evolution to begin. If no Cannizzaro reaction was involved, aldehyde oxidation would initiate immediately. This delay is apparently benzaldehyde disproportionation that is required to generate a sufficient amount of benzyl alcohol to form the catalytic species. We expect that it is required to convert **1** to **1a** (and **2** to **2a**), and that its C—H groups are needed to convert on to **1b** (or **2b**): an aldehyde cannot fill this role. After hydrogen formation ceases, traces of benzyl alcohol can be detected in the reaction mixture by ¹H NMR spectroscopy. These observations necessitate Cannizzaro reaction, but do not necessitate or exclude Tishchenko reaction in the sequence.

SUMMARY

In conclusion, complexes **1** and **2** are efficient pre-catalysts for the conversion of primary alcohols to potassium carboxylates. Under optimized the reaction conditions the method applicable to a wide range of substrates, including some (amino alcohols and some heterocycles) that are unknown for any catalytic conditions in this class. We show that **1** and **2** are both active in primary alcohol dehydrogenation, despite their previously investigated difference in catalytic activity towards glycerol and formic acid dehydrogenation. Upon catalysis initiation, complex **1** forms observable iridium(I) alkoxide **1a**, which decomposes to relatively reactive iridium hydrides. On the contrary, complex **2** reacts with alcohols in the presence of KOH to form a number of stable iridium hydride complexes **2b**, **2c**, **2f**, and **2g** even though **2a** is not observed. We propose that the jumping-off point for catalysis to be an intermediate in the equilibration of **2c** and **2g**.

Taken together with our prior work on glycerol and formic acid dehydrogenation, realized respectively with **1** and **2**, these data help to frame a picture that explains the specificity of **1** and **2** for those processes: both proceed through initiation sequences that are differentiated by the reactivities of intermediate iridium hydride intermediates that steer initiation to the respective active species. These stabilities are apparently governed by differences in metal-ligand bonding between NHC carbene and phosphine groups, thus illustrating dramatic consequences manifested by the subtle differences in these ligating moieties. More details on this generalization are forthcoming from our lab.

EXPERIMENTAL SECTION

Materials and Methods

Chloroform-*d*₁, dimethyl sulfoxide-*d*₆, methanol-*d*₄, D₂O, benzene-*d*₆, and toluene-*d*₈ were purchased from Cambridge Isotopes Laboratories. Benzene-*d*₆, toluene-*d*₈, and toluene were dried and distilled according to known procedures. Iridium complexes **1**, **2**, **3**, and **4** were synthesized according to described procedures.^{20,21} Alcohols **6a** – **6r**, methanol, isopropanol, dichloromethane, ethyl acetate, methyl hexanoate, 18-crown-6, chloro(1,5-

cyclooctadiene)iridium(I) dimer, and potassium hydroxide were purchased from commercial sources without further purification. Benzaldehyde was distilled under reduced pressure prior to use. All air and water sensitive procedures were carried out in a Vacuum Atmosphere glove box under nitrogen (2-10 ppm O₂ for all manipulations). ¹H, ¹³C, ³¹P NMR spectra were recorded on Varian Mercury 400 and VNMRS 600 spectrometers, and processed using MestReNova v11.0.2. All chemical shifts are reported in ppm and referenced to the residual ¹H or ¹³C solvent peaks. Following abbreviations are used: (s) singlet, (bs s) broad singlet, (d) doublet, (t) triplet, (dd) double doublet, etc. NMR spectra of air-sensitive compounds were taken in 8" J. Young tubes (Wilmad or Norell) with Teflon valve plugs. Infrared spectra were recorded on Bruker OPUS FTIR spectrometer. Samples of pure potassium carboxylates were treated with acetic acid in ethyl acetate followed by GC-MS analysis on Thermo Scientific Focus DSQ II instrument. MALDI-MS spectra were acquired on Bruker Autoflex Speed MALDI Mass Spectrometer. Elemental analyses were conducted on Flash 2000 CHNS Elemental Analyzer.

General Procedure for Alcohol Dehydrogenation

An alcohol (2.0 mmol), iridium complex **1** or **2** (see table 2), and potassium hydroxide (123 mg, 2.2 mmol) were mixed with dry toluene (10 mL). The suspension was stirred at reflux for required period of time (oil bath, 120 °C). After the reaction was over, the solvent was evaporated under reduced pressure affording crude potassium carboxylate.

Isolation method A—Potassium carboxylate was dissolved in deionized water (40 mL) and the resulting solution was washed with dichloromethane (2 × 10 mL). Then, the solution was acidified with 1 M HCl, and extracted with ethyl acetate (3 × 10 mL). The organic phase was separated, dried (Na₂SO₄) and evaporated in vacuum, giving pure carboxylic acid.

Isolation method B—Potassium carboxylate was dissolved in DI water (40 mL) and the resulting solution was washed with dichloromethane (2 × 10 mL). The aqueous solution was evaporated in vacuum to dryness and the residue was dissolved in methanol. The methanol solution was filtered, and the filtrate was evaporated to dryness, giving pure potassium carboxylate.

Potassium Butyrate (7a)

Potassium Butyrate (**7a**) was isolated by method B as a white powder (0.24 g, 96%). ¹H NMR (600 MHz, D₂O): δ 2.16 (t, *J* = 7.3 Hz, 2H, CH₂), 1.57 (h, *J* = 7.3 Hz, 2H, CH₂), 0.90 (t, *J* = 7.4 Hz, 3H, CH₃). ¹³C NMR (151 MHz, D₂O): δ 184.05, 39.64, 19.35, 13.26. IR (PE film, cm⁻¹): 2956, 2918, 1564, 1412, 1254, 888, 750. GC-MS: *m/z* calcd. for C₄H₈O₂ [M]⁺ 88.05, found 88.1.

Potassium Octanoate (7b)

Potassium Octanoate (**7b**) was isolated by method B as a white powder (0.33 g, 90%). ¹H NMR (400 MHz, D₂O): δ 2.18 (t, *J* = 7.5 Hz, 2H, CH₂), 1.63 – 1.47 (m, 2H, CH₂), 1.38 – 1.20 (m, 8H, 4CH₂), 0.88 (t, *J* = 6.7 Hz, 3H, CH₃). ¹³C NMR (100 MHz, D₂O): δ 184.13, 37.50, 30.88, 28.55, 28.09, 25.75, 21.83, 13.24. IR (KBr, cm⁻¹): 2954, 2926, 2854, 1563, 1411, 914, 718, 694. GC-MS: *m/z* calcd. for C₈H₁₆O₂ [M]⁺ 144.12, found 144.1.

Potassium Palmitate (7c)

After evaporation of toluene, crude **7c** was washed with hexanes and dried under reduced pressure. White powder (0.50 g, 85%). ^1H NMR (600 MHz, CD_3OD): δ 2.15 (t, J = 8.6 Hz, 2H, CH_2), 1.63 – 1.55 (m, 2H, CH_2), 1.35 – 1.25 (m, 24H, 12CH_2), 0.90 (t, J = 7.0 Hz, 3H, CH_3). ^{13}C NMR (151 MHz, CD_3OD): δ 183.12, 39.38, 33.07, 30.90, 30.79 (6CH_2), 30.76, 30.68, 30.47, 27.85, 23.73, 14.45. IR (PE film, cm^{-1}): 2925, 2850, 1561, 1472, 1331, 1104, 716. GC-MS: m/z calcd. for $\text{C}_{16}\text{H}_{32}\text{O}_2$ $[\text{M}]^+$ 256.24, found 256.3.

Potassium Cyclobutanecarboxylate (7d)

Potassium Cyclobutanecarboxylate (**7d**) was isolated by method B as a white powder (0.22 g, 81%). ^1H NMR (600 MHz, D_2O): δ 3.03 (p, J = 8.7 Hz, 1H, CH), 2.15 – 2.05 (m, 4H, 2CH_2), 1.89 (h, J = 9.2 Hz, 1H, CH_2), 1.78 – 1.70 (m, 1H, CH_2). ^{13}C NMR (151 MHz, D_2O): δ 185.74, 40.92, 25.93, 17.29. IR (PE film, cm^{-1}): 2975, 2941, 2859, 1656, 1553, 1409, 680. GC-MS: m/z calcd. for $\text{C}_5\text{H}_8\text{O}_2$ $[\text{M}]^+$ 100.05, found 100.1.

1-Adamantanecarboxylic Acid (7e)

Isolation by method A followed by recrystallization from hexane-ethanol mixture gave **7e** as colorless crystals (0.34 g, 77%). ^1H NMR (600 MHz, CDCl_3): δ 2.00 – 2.05 (m, 3H, 3CH), 1.88 – 1.94 (m, 6H, 3CH_2), 1.67 – 1.77 (m, 6H, 3CH_2). ^{13}C NMR (151 MHz, CDCl_3): δ 184.45, 40.64, 38.71, 36.57, 27.97. IR (PE film, cm^{-1}): 2928, 1693, 1450, 1410, 1284, 1085, 951, 744, 670, 531. GC-MS: m/z calcd. for $\text{C}_{11}\text{H}_{16}\text{O}_2$ $[\text{M}]^+$ 180.12, found 180.1.

Benzoic Acid (7f)

Isolation by method A followed by recrystallization from toluene gave **7f** as colorless crystals (0.24 g, 98%). ^1H NMR (600 MHz, $\text{DMSO}-d_6$): δ 12.93 (br s, 1H, CO_2H), 7.95 (d, J = 7.0 Hz, 2H, 2CH), 7.62 (t, J = 7.4 Hz, 1H, CH), 7.50 (t, J = 7.7 Hz, 2H, 2CH). ^{13}C NMR (151 MHz, $\text{DMSO}-d_6$): δ 167.33, 132.88, 130.76, 129.27, 128.58. IR (PE film, cm^{-1}): 1689, 1455, 1426, 1327, 1294, 936, 709. GC-MS: m/z calcd. for $\text{C}_7\text{H}_6\text{O}_2$ $[\text{M}]^+$ 122.04, found 122.0.

4-Methoxybenzoic Acid (7g)

Isolation by method A followed by recrystallization from toluene-ethanol mixture gave **7g** as colorless crystals (0.24 g, 79%). ^1H NMR (600 MHz, $\text{DMSO}-d_6$): δ 12.62 (br s, 1H, CO_2H), 7.89 (d, J = 8.7 Hz, 2H, 2CH), 7.01 (d, J = 8.7 Hz, 2H, 2CH), 3.81 (s, 3H, CH_3). ^{13}C NMR (151 MHz, $\text{DMSO}-d_6$): δ 167.04, 162.86, 131.37, 123.00, 113.83, 55.45. IR (PE film, cm^{-1}): 1683, 1603, 1427, 1301, 1263, 1168, 1026, 927, 844, 773, 617, 550. GC-MS: m/z calcd. for $\text{C}_8\text{H}_8\text{O}_3$ $[\text{M}]^+$ 152.05, found 152.0.

4-(Methylthio)benzoic Acid (7h)

Isolation by method A followed by recrystallization from toluene-ethanol mixture gave **7h** as colorless crystals (0.25 g, 74%). ^1H NMR (500 MHz, CD_3OD): δ 7.92 (d, J = 7.9 Hz, 2H, 2CH), 7.30 (d, J = 8.1 Hz, 2H, 2CH), 2.52 (s, 3H, CH_3). ^{13}C NMR (126 MHz, CD_3OD): δ 169.62, 147.25, 131.07, 127.81, 125.94, 14.66. IR (KBr, cm^{-1}): 1680, 1595, 1421, 1325, 1192, 757. GC-MS: m/z calcd. for $\text{C}_8\text{H}_8\text{O}_2\text{S}$ $[\text{M}]^+$ 168.02, found 168.0.

4-Chlorobenzoic Acid (7i)

Isolation by method A followed by recrystallization from toluene-ethanol mixture gave **7i** as colorless crystals (0.25 g, 80%). ^1H NMR (400 MHz, DMSO- d_6): δ 13.09 (br s, 1H, CO₂H), 7.93 (d, J = 8.5 Hz, 2H, 2CH), 7.55 (d, J = 8.5 Hz, 2H, 2CH). ^{13}C NMR (151 MHz, DMSO- d_6): δ 166.49, 137.83, 131.16, 129.67, 128.75. IR (KBr, cm^{-1}): 2924, 2955, 1680, 1322, 1284, 762. GC-MS: m/z calcd. for C₇H₅ClO₂ [M]⁺ 156.00, 157.99; found 156.0, 158.0.

4-Bromobenzoic Acid (7j)

Isolation by method A followed by recrystallization from toluene-ethanol mixture gave **7j** as colorless crystals (0.16 g, 40%). ^1H NMR (600 MHz, DMSO- d_6): δ 13.17 (s, 1H, CO₂H), 7.86 (d, J = 7.1 Hz, 2H, 2CH), 7.70 (d, J = 7.1 Hz, 2H, 2CH). ^{13}C NMR (151 MHz, DMSO- d_6): δ 166.58, 131.68, 131.27, 130.00, 126.85. IR (PE film, cm^{-1}): 1676, 1587, 1426, 1320, 1070, 1013, 758. GC-MS: m/z calcd. for C₇H₅BrO₂ [M]⁺ 199.95, 201.95; found 199.9, 201.9.

4-Iodobenzoic Acid (7k)

Isolation by method A followed by recrystallization from toluene-ethanol mixture gave **7k** as colorless crystals (0.21 g, 42%). ^1H NMR (600 MHz, DMSO- d_6): δ 13.12 (s, 1H, CO₂H), 7.88 (d, J = 8.1 Hz, 2H, 2CH), 7.69 (d, J = 8.0 Hz, 2H, 2CH). ^{13}C NMR (151 MHz, DMSO- d_6): δ 166.88, 137.55, 131.04, 130.27, 101.14. IR (PE film, cm^{-1}): 1675, 1427, 1009, 754. MALDI-MS: m/z calcd. for C₇H₅IO₂ [M + Na]⁺ 270.92, found 270.72.

1-Naphthoic Acid (7l)

Isolation by method A followed by recrystallization from toluene gave **7l** as colorless crystals (0.29 g, 84%). ^1H NMR (600 MHz, DMSO- d_6): δ 13.14 (s, 1H, CO₂H), 8.87 (d, J = 8.6 Hz, 1H, CH), 8.15 (d, J = 7.4 Hz, 2H, 2CH), 8.01 (d, J = 8.0 Hz, 1H, CH), 7.64 (t, J = 7.7 Hz, 1H, CH), 7.59 (t, J = 7.7 Hz, 2H, 2CH). ^{13}C NMR (151 MHz, DMSO- d_6): δ 168.65, 133.46, 132.92, 130.67, 129.84, 128.59, 127.71, 127.55, 126.17, 125.48, 124.87. IR (PE film, cm^{-1}): 2916, 1674, 1593, 1306, 774. MALDI-MS: m/z calcd. for C₁₁H₈NaO₂ [M + Na]⁺ 195.04, found 194.87.

Potassium Ethylaminoacetate (7m)

Potassium Ethylaminoacetate (**7m**) isolated by method B as a white powder (0.23 g, 82%). ^1H NMR (600 MHz, D₂O): δ 3.26 (s, 2H, CH₂), 2.70 (q, J = 6.8 Hz, 2H, CH₂), 1.13 (t, J = 7.1 Hz, 3H, CH₃). ^{13}C NMR (151 MHz, D₂O): δ 177.81, 51.11, 42.62, 12.90. IR (PE film, cm^{-1}): 1597, 1407, 1383, 1283. MALDI-MS: m/z calcd. for C₄H₈K₂NO₂ [M + K]⁺ 179.98, found 180.00.

Indole (7n)

Complex **2** (2.7 mg, 4 μmol), **6n** (274 mg, 2.0 mmol), and potassium hydroxide (123 mg, 2.2 mmol) were mixed with dry toluene (10 mL). The suspension was stirred at reflux for 13 hours (oil bath, 120 °C). After the reaction was over, the solvent was evaporated in vacuum, and the residue was stirred at reflux with hexanes (50 mL) and charcoal for 1 h. Then, the hexane solution was filtered and evaporated in vacuum giving **7n** as a colorless liquid (0.19

g, 80%). ^1H NMR (600 MHz, CDCl_3): δ 8.11 (br s, 1H, NH), 7.68 (dd, $J = 7.8, 0.7$ Hz, 1H, CH), 7.41 (dd, $J = 8.0, 0.7$ Hz, 1H, CH), 7.25 – 7.19 (m, 2H, 2CH), 7.17 – 7.12 (m, 1H, CH), 6.60 – 6.56 (m, 1H, CH). ^{13}C NMR (151 MHz, CDCl_3): δ 135.88, 127.95, 124.25, 122.09, 120.84, 119.92, 111.14, 102.71. IR (PE film, cm^{-1}): 3401, 1457, 1353, 1246, 1090, 932, 746, 612, 505, 430. GC-MS: m/z calcd. for $\text{C}_8\text{H}_7\text{N}$ $[\text{M}]^+$ 117.06, found 117.1.

3-Phenylpropanoic Acid (7o)

Isolation by method A gave **7o** as a yellow liquid (0.24 g, 80%). ^1H NMR (600 MHz, CDCl_3): δ 11.57 (br s, 1H, CO_2H), 7.34 – 7.29 (m, 2H, 2CH), 7.25 – 7.20 (m, 3H, 3CH), 2.99 (t, $J = 7.8$ Hz, 2H, CH_2), 2.71 (t, $J = 7.8$ Hz, 2H, CH_2). ^{13}C NMR (151 MHz, CDCl_3): δ 179.50, 140.27, 128.70, 128.39, 126.51, 35.77, 30.71. IR (PE film, cm^{-1}): 3028, 1708, 1496, 1417, 1295, 1215, 936, 748, 699. GC-MS: m/z calcd. for $\text{C}_9\text{H}_{10}\text{O}_2$ $[\text{M}]^+$ 150.07, found 150.1.

Potassium Pyridine-2-carboxylate (7p)

Potassium Pyridine-2-carboxylate (**7p**) was isolated by method B as a white powder (0.20 g, 63%). ^1H NMR (500 MHz, CD_3OD): δ 8.58 (d, $J = 4.4$ Hz, 1H, CH), 8.02 (d, $J = 7.7$ Hz, 1H, CH), 7.85 (t, $J = 8.1$ Hz, 1H, CH), 7.46 – 7.32 (m, 1H, CH). ^{13}C NMR (126 MHz, CD_3OD): δ 172.94, 156.47, 149.55, 138.17, 125.93, 125.01. IR (KBr, cm^{-1}): 2927, 1640, 1405, 702. GC-MS: m/z calcd. for $\text{C}_6\text{H}_5\text{NO}_2$ $[\text{M}]^+$ 123.03, found 123.0.

Potassium Quinoline-2-carboxylate (7q)

Potassium Quinoline-2-carboxylate (**7q**) was isolated by method B as a white powder (0.27 g, 65%). ^1H NMR (600 MHz, D_2O): δ 7.88 (d, $J = 8.5$ Hz, 1H, CH), 7.77 (d, $J = 8.5$ Hz, 1H, CH), 7.60 (d, $J = 8.4$ Hz, 1H, CH), 7.50 (t, $J = 7.7$ Hz, 1H, CH), 7.45 (d, $J = 8.1$ Hz, 1H, CH), 7.28 (t, $J = 7.5$ Hz, 1H, CH). ^{13}C NMR (151 MHz, D_2O): δ 172.84, 154.01, 145.89, 137.75, 130.12, 128.09, 127.96, 127.60, 127.38, 120.13. IR (KBr, cm^{-1}): 3298, 1615, 1387, 802, 770. GC-MS: m/z calcd. for $\text{C}_9\text{H}_7\text{N}$ $[\text{M} - \text{CO}_2]^+$ 129.16, found 129.1.

1-Hexanol-O,1,1- d_3 (6s)

In a glovebox, a solution of methyl hexanoate (2.06 g, 15.8 mmol) in 10 mL of dry ether was added drop-wise to a stirred solution of LiAlD_4 (0.67 g, 15.8 mmol) in 20 mL of ether. The mixture was stirred at room temperature for 24 h, and then carefully quenched with D_2O at vigorous stirring till aluminum hydroxide separated from organic phase. The ethereal solution was separated, dried (Na_2SO_4), and evaporated in vacuum. The product was obtained as a colorless liquid (1.34 g, 81%). ^1H NMR (600 MHz, CDCl_3): δ 1.52 (t, $J = 7.8$ Hz, 2H, CH_2), 1.34 – 1.24 (m, 6H, 3 CH_2), 0.87 (t, $J = 7.0$ Hz, 3H, CH_3). ^{13}C NMR (151 MHz, CDCl_3): δ 62.13 (p, $^1J_{\text{CD}} = 21.5$ Hz), 32.58, 31.76, 25.49, 22.73, 14.10. IR (PE film, cm^{-1}): 3331, 2957, 2859, 1467, 1160, 1127, 967. GC-MS: m/z calcd. for $\text{C}_6\text{H}_{10}\text{D}_2$ $[\text{M} - \text{HDO}]^+$ 86.11, found 86.1.

$[\text{Ir}(\text{2-PyCH}_2(\text{C}_4\text{H}_5\text{N}_2))(\eta^2\text{-COD})(\text{OCH}_2\text{C}_6\text{H}_4\text{OMe})]$ (1a)

In a glovebox, complex **1** (40.0 mg, 6.4×10^{-5} mol), **6g** (18.0 mg, 1.3×10^{-4} mol), potassium hydroxide (7.2 mg, 1.3×10^{-4} mol) and 2 – 3 drops of C_6D_6 were mixed together

till the slurry turned yellow. Then, C₆D₆ (0.7 mL) was added resulting in a yellow solution of **1a** and potassium triflate precipitate. The solution was immediately filtered and transferred to J. Young NMR tube. The structure of **1a** was derived from NMR data. ¹H NMR (600 MHz, C₆D₆): δ 8.33 (dq, *J* = 5.0, 0.9 Hz, 1H, Py), 7.39 (d, *J* = 7.8 Hz, 1H, Py), 7.35 (d, *J* = 8.6 Hz, 2H, C₆H₄), 7.08 (td, *J* = 7.7, 1.8 Hz, 1H, Py), 6.85 (d, *J* = 8.6 Hz, 2H, C₆H₄), 6.64 (d, *J* = 1.9 Hz, 1H, NHC), 6.58 (ddd, *J* = 7.5, 4.8, 1.1 Hz, 1H, Py), 5.86 (d, *J* = 1.9 Hz, 1H, NHC), 5.73 (d, *J* = 14.7 Hz, 1H, NCH₂), 5.42 (d, *J* = 14.7 Hz, 1H, NCH₂), 5.24 (d, *J* = 13.8 Hz, 1H, OCH₂), 5.10 (td, *J* = 7.7, 3.6 Hz, 1H, =CH), 5.00 – 5.06 (m, 1H, =CH), 4.85 (d, *J* = 13.7 Hz, 1H, OCH₂), 3.40 (s, 3H, OCH₃), 3.19 (s, 3H, NCH₃), 2.49 (td, *J* = 7.0, 2.4 Hz, 1H, =CH), 2.41 (td, *J* = 7.4, 3.0 Hz, 1H, =CH), 2.28 – 2.37 (m, 3H, 2CH₂), 2.11 – 2.17 (m, 1H, CH₂), 1.62 – 1.83 (m, 4H, 2CH₂). ¹³C NMR (151 MHz, C₆D₆, derived from HSQC and HMBC): δ 183.25, 158.69, 156.75, 149.34, 141.45, 136.46, 127.26, 123.17, 122.46, 120.82, 120.56, 113.36, 84.78, 84.04, 75.30, 55.27, 54.66, 45.81, 45.44, 36.38, 34.54, 33.77, 29.90, 29.23. MALDI-MS: *m/z* calcd. for C₂₆H₃₂IrN₃O₂ [M]⁺ 611.21, found 611.14.

Decomposition of **1a** to **1b** and **1c**

Complex **1a** is unstable in a solution, and it completely decomposes in two days to **1b**, **1c**, and iridium-containing precipitate. **1b**: ¹H NMR (600 MHz, C₆D₆): δ 8.16 (d, *J* = 9.0 Hz, 2H, 2CH), 7.21 (d, *J* = 8.8 Hz, 2H, 2CH), 6.73 (d, *J* = 8.7 Hz, 2H, 2CH), 6.62 (d, *J* = 9.0 Hz, 2H, 2CH), 5.23 (s, 2H, CH₂), 3.26 (s, 3H, CH₃), 3.13 (s, 3H, CH₃). GC-MS: *m/z* calcd. for C₁₆H₁₆O₄ [M]⁺ 272.10, found 272.1. **1c**: ¹H NMR (600 MHz, C₆D₆): δ 5.62 – 6.67 (m, 2H, 2CH), 2.02 – 2.12 (m, 4H, 2CH₂), 1.36 – 1.48 (m, 8H, 4CH₂). GC-MS: *m/z* calcd. for C₈H₁₄ [M]⁺ 110.11, found 110.1.

[IrH(η¹, η³-C₈H₁₂)(2-PyCH₂PBu₂^t)] (**2b**)

In a glovebox, complex **2** (50.0 mg, 7.3 × 10⁻⁵ mol), isopropyl alcohol (20.0 mg, 3.3 × 10⁻⁴ mol), and potassium hydroxide (12.0 mg, 2.2 × 10⁻⁴ mol) were mixed with dry benzene (1.0 mL) and stirred at room temperature for two days. Then, the brown solution was filtered and the solvent was evaporated in vacuum to dryness. The residue was recrystallized twice from benzene affording the product as a pale-yellow crystalline powder (25.0 mg, 64%). Crystals suitable for X-ray analysis were obtained by slow evaporation of benzene solution. ¹H NMR (600 MHz, C₆D₆): δ 7.77 (d, *J* = 5.6 Hz, 1H, Py), 6.65 (t, *J* = 7.3 Hz, 1H, Py), 6.44 (d, *J* = 7.5 Hz, 1H, Py), 6.05 (t, *J* = 6.4 Hz, 1H, Py), 5.20 – 5.13 (m, 1H, CH), 4.64 – 4.57 (m, 1H, CH), 3.91 (t, *J* = 7.8 Hz, 1H, CH), 2.96 – 2.90 (m, 1H, CH), 2.87 (dd, *J* = 16.6, 9.0 Hz, 1H, PCH₂), 2.68 (dd, *J* = 16.6, 8.2 Hz, 1H, PCH₂), 2.62 – 2.51 (m, 1H, CH₂), 2.27 – 2.11 (m, 4H, 3CH₂), 2.05 – 1.99 (m, 1H, CH₂), 1.94 – 1.77 (m, 2H, 2CH₂), 1.38 (d, *J* = 12.1 Hz, 9H, 3CH₃), 1.10 (d, *J* = 12.3 Hz, 9H, 3CH₃), -9.99 (d, *J* = 17.6 Hz, 1H, IrH). ¹³C NMR (151 MHz, C₆D₆): δ 163.78, 148.87, 133.73, 121.87, 121.10, 96.21, 76.00, 60.79, 56.43, 55.14, 38.75, 36.48, 35.29, 30.34, 29.06, 28.05, 25.33, 14.01. ³¹P{¹H} NMR (243 MHz, C₆D₆): δ 56.20. IR (KBr, cm⁻¹): 2915, 2871, 2800, 2043, 1472, 821, 762. MALDI-MS: *m/z* calcd. for C₂₂H₃₇IrNP [M]⁺ 539.23, found 539.31. Anal. calcd for C₂₂H₃₇IrNP: C 49.05, H 6.92, N 2.60. Found: C 48.11, H 6.96, N 2.76.

[Ir₂H₃(CO)(2-PyCH₂PBu₂[†]){μ-(C₅H₃N)CH₂P[†]Bu₂}] (2c)

In a glovebox, complex **2** (50.0 mg, 7.3×10^{-5} mol), *n*-butanol (108.0 mg, 1.46×10^{-3} mol, 20 eq.), and potassium hydroxide (88.0 mg, 1.57×10^{-3} mol, 21.5 eq.) were mixed with dry toluene (5 mL) in a 20 mL Straus flask. The flask was charged with a stirring bar and sealed with a septum. Outside the glovebox, the flask was placed in an oil bath (120 °C), and the septum was immediately pierced with a syringe needle attached to eudiometer. In 15 min hydrogen evolution stopped, and the solution color turned from dark-violet to orange. The flask was brought back to the glovebox, and the precipitate (potassium butyrate) was filtered off and washed with toluene. The orange solution was evaporated to dryness under vacuum, and then hexane (3 mL) was added to the solid to form a yellow precipitate. The precipitate was filtered and washed with hexane. After crystallization from benzene-hexane mixture, **2c** was obtained as a yellow crystalline powder (20 mg, 63%). Crystals suitable for X-ray analysis were obtained by slow addition of hexane to benzene solution. ¹H NMR (600 MHz, C₆D₆): δ 8.58 (d, *J* = 5.6 Hz, 1H, ArH), 7.90 (dd, *J* = 7.7, 2.1 Hz, 1H, ArH), 6.86 (t, *J* = 7.6 Hz, 1H, ArH), 6.78 (td, *J* = 7.5, 1.3 Hz, 1H, ArH), 6.62 (d, *J* = 7.8 Hz, 1H, ArH), 6.51 (d, *J* = 7.4 Hz, 1H, ArH), 6.07 (t, *J* = 7.1 Hz, 1H, ArH), 3.19 (dd, *J* = 15.7, 7.7 Hz, 1H, CH₂), 3.00 (dd, *J* = 15.8, 7.3 Hz, 1H, CH₂), 2.58 – 2.43 (m, 2H, CH₂), 1.50 (d, *J* = 12.2 Hz, 9H, 3CH₃), 1.37 (d, *J* = 12.1 Hz, 9H, 3CH₃), 1.18 (d, *J* = 13.6 Hz, 9H, 3CH₃), 1.11 (d, *J* = 13.4 Hz, 9H, 3CH₃), -7.51 (dd, *J* = 67.6, 7.5 Hz, 1H, IrH), -13.87 (ddd, *J* = 26.7, 13.7, 5.3 Hz, 1H, IrH), -19.99 (dt, *J* = 12.2, 4.1 Hz, 1H, IrH). ¹³C NMR (151 MHz, C₆D₆): δ 187.12 (d, *J* = 8.0 Hz), 178.55 (dd, *J* = 103.5, 4.4 Hz), 166.04 (d, *J* = 6.2 Hz), 164.98 (dd, *J* = 10.8, 6.1 Hz), 153.04 (d, *J* = 2.5 Hz), 144.85 (d, *J* = 7.7 Hz), 134.48, 133.03 (d, *J* = 4.6 Hz), 121.93 (d, *J* = 7.3 Hz), 120.35, 112.56 (d, *J* = 9.2 Hz), 39.69 (d, *J* = 16.1 Hz), 35.21 (d, *J* = 15.4 Hz), 35.06 (d, *J* = 13.5 Hz), 34.71 (d, *J* = 12.0 Hz), 33.14 (d, *J* = 19.0 Hz), 30.92 (d, *J* = 23.9 Hz), 30.59 – 30.08 (m), 29.87 (d, *J* = 4.6 Hz), 29.61 – 28.98 (m). ³¹P{¹H} NMR (243 MHz, C₆D₆): δ 89.01, 62.75. IR (KBr, cm⁻¹): 2942, 2896, 2106, 1914, 1582, 1473, 826. MALDI-MS: *m/z* calcd. for C₂₉H₅₀Ir₂N₂OP₂ [M]⁺ 888.26, found 888.23. Anal. calcd for C₂₉H₅₀Ir₂N₂OP₂: C 39.18, H 5.67, N 3.15. Found: C 39.91, H 5.71, N 3.19.

Conversion of 2b to 2d

A solution of **2b** (10 mg) and sodium formate (10 mg) in formic acid (0.7 mL) was placed in a J. Young NMR tube. The tube was connected to eudiometer and heated in an oil bath at 70 °C for 30 min. About 15 mL of gas was produced during heating. The solvent was evaporated in vacuum and the resulting residue was left under vacuum for 1 h. The residue was then dissolved in formic acid-*d*₂. ¹H NMR spectrum of the residue contains peaks at -19.39, -25.04, and -27.11 ppm which were assigned to complex **2d**.²⁰

Isomerization of 2c to 2f

A solution of **2c** (40 mg) in toluene-*d*₈ (0.7 mL) was placed in a J. Young NMR tube and heated in an oil bath at 110 °C for 4 h. The resulting solution contained **2c** and **2f** in a 1.6 : 1 ratio (*K*_{eq} = 0.626). The structure of **2f** was derived from NMR data: ¹H NMR (600 MHz, toluene-*d*₈): δ 9.41 (d, *J* = 6.7 Hz, 1H, ArH), 7.26 (d, *J* = 8.0 Hz, 1H, ArH), 6.74 (td, *J* = 7.7, 1.6 Hz, 1H, ArH), 6.61 (d, *J* = 7.8 Hz, 1H, ArH), 6.55 (t, *J* = 7.3 Hz, 1H, ArH), 6.20 (d, *J* = 7.3 Hz, 1H, ArH), 5.98 (t, *J* = 7.2 Hz, 1H, ArH), 3.02 (d, *J* = 7.8 Hz, 2H, CH₂), 2.52 (d, *J* =

8.7 Hz, 2H, CH₂), 1.30 (d, $J = 12.2$ Hz, 18H, 6CH₃), 1.23 (d, $J = 13.4$ Hz, 18H, 6CH₃), -6.64 (d, $J = 150.4$ Hz, 1H, IrH), -8.98 (br s, 2H, 2IrH, resolves to a doublet at 100 °C with $J = 46.2$ Hz). ¹³C NMR (151 MHz, toluene-*d*₈, derived from HSQC and HMBC): δ 164.19, 163.48, 162.13, 159.87, 140.85, 134.09, 131.10, 121.13, 120.70, 109.83, 39.65, 34.44, 34.03, 31.80. ³¹P{¹H} NMR (243 MHz, toluene-*d*₈): δ 88.66, 63.79.

Deuteration of **2c** under Alcohol Dehydrogenation Conditions

In a glovebox, complex **2c** (10.0 mg, 1.13×10^{-5} mol), 1-hexanol-*O*,1,1-*d*₃ (59.0 mg, 5.62×10^{-4} mol, 50 eq.), and potassium hydroxide (31.0 mg, 5.62×10^{-4} mol, 50 eq.) were mixed with dry toluene (5 mL) in a 20 mL Straus flask. The following manipulations were the same as in the synthesis of **2c** (reaction time was 3 h). Analysis of the recovered **2c-d**₄ by ¹H NMR spectroscopy showed partial deuteration (up to 34%) of protons with chemical shifts at 6.62, -7.51, -13.87, and -19.99 ppm.

Conversion of **2c** to **2g**

A solution of **2c** (20.0 mg, 2.25×10^{-5} mol) and freshly distilled *n*-hexanal (22.5 mg, 2.25×10^{-4} mol, 10 eq.) in C₆D₆ (0.5 mL) was placed in a J. Young NMR tube and heated in an oil bath at 80 °C for two days. The resulting solution contained **2g**, *n*-hexanol, hexyl hexanoate, and unreacted *n*-hexanal. The solution was evaporated to dryness under vacuum giving crude **2g** as a dark-yellow oil. The structure of **2g** was derived from NMR data: ¹H NMR (600 MHz, toluene-*d*₈): δ 8.18 (dd, $J = 4.7, 1.7$ Hz, 1H, ArH), 7.43 (dd, $J = 7.6, 2.6$ Hz, 1H, ArH), 6.81 (t, $J = 7.6$ Hz, 1H, ArH), 6.76 (dd, $J = 7.5, 1.8$ Hz, 1H, ArH), 6.53 (d, $J = 7.5$ Hz, 1H, ArH), 6.36 (dd, $J = 7.5, 4.7$ Hz, 1H, ArH), 3.76 (dd, $J = 16.6, 9.2$ Hz, 1H, CH₂), 3.60 (dd, $J = 16.6, 9.5$ Hz, 1H, CH₂), 2.41 (d, $J = 8.7$ Hz, 2H, CH₂), 1.37 (d, $J = 13.1$ Hz, 9H, 3CH₃), 1.20 (d, $J = 12.8$ Hz, 9H, 3CH₃), 1.06 (d, $J = 13.9$ Hz, 9H, 3CH₃), 0.96 (d, $J = 14.0$ Hz, 9H, 3CH₃), -8.44 (ddd, $J = 52.5, 7.3, 5.2$ Hz, 1H, IrH), -11.15 (ddd, $J = 25.9, 12.6, 5.2$ Hz, 1H, IrH). ³¹P{¹H} NMR (243 MHz, toluene-*d*₈): δ 88.18, 44.46. MALDI-MS: *m/z* calcd. for C₂₉H₄₈Ir₂N₂OP₂ [M]⁺ 886.25, found 886.25.

Deprotonation of **2c**

t-BuOK (12.6 mg, 1.13×10^{-4} mol, 5 eq.) was added to a solution of **2c** (20.0 mg, 2.25×10^{-5} mol) in C₆D₆ (0.5 mL) which caused formation of **2h** and instant color change from yellow to dark-red. Addition of *n*-hexanol (23.0 mg, 2.25×10^{-4} mol, 10 eq.) to the red solution converted **2h** back to **2c**. These transformations were monitored by ¹H NMR (see Supporting Information).

Supplementary Material

Refer to Web version on PubMed Central for supplementary material.

Acknowledgments

This work is sponsored by the NSF (CHE-1566167), and the Hydrocarbon Research Foundation. We thank the NSF (DBI-0821671, CHE-0840366, CHE-1048807) and the NIH (S10 RR25432) for analytical instrumentation. We thank Prof. Ralf Haiges for help with X-ray crystallography. Fellowship assistance from USC Dornsife College is gratefully acknowledged.

References

1. Fatiadi AJ. The Classical Permanganate Ion: Still a Novel Oxidant in Organic Chemistry. *Synthesis*. 1987; 2:85–127.
2. Lee DG, Ribagorda M, Adrio J. “Potassium Permanganate” *Encyclopedia of Reagents for Organic Synthesis*. John Wiley & Sons, Ltd; 2001.
3. Freeman F. “Chromic Acid” *Encyclopedia of Reagents for Organic Synthesis*. John Wiley & Sons, Ltd; 2001.
4. Piancatelli G. “Pyridinium Dichromate” *Encyclopedia of Reagents for Organic Synthesis*. John Wiley & Sons, Ltd; 2001.
5. Martin VS, Palazon JM, Rodriguez CM, Nevill CR, Hutchinson DK. “Ruthenium(VIII) Oxide” *Encyclopedia of Reagents for Organic Synthesis*. John Wiley & Sons, Ltd; 2001.
6. Galvin JM, Jacobsen EN, Palucki M, Frederick MO. “Sodium Hypochlorite” *Encyclopedia of Reagents for Organic Synthesis*. John Wiley & Sons, Ltd; 2001.
7. Reid EE, Worthington H, Larchar AW. The Action of Caustic Alkali and of Alkaline Salts on Alcohols. *J Am Chem Soc*. 1939; 61:99–101.
8. Ciufolini MA, Swaminathan S. Synthesis of a Model Depsipeptide Segment of Luzopeptins (BBM 928), Potent Antitumor and Antiretroviral Antibiotics. *Tetrahedron Lett*. 1989; 30:3027–3028.
9. Crimmins MT, DeBaillie AC. Enantioselective Total Synthesis of Bistramide A. *J Am Chem Soc*. 2006; 128:4936–4937. [PubMed: 16608311]
10. Salunke GB, Shivakumar I, Gurjar MK. Total Synthesis of Verbalactone: an Efficient, Carbohydrate-Based Approach. *Tetrahedron Lett*. 2009; 50:2048–2049.
11. Fuwa H. Chapter 5 - (–)-Lyngbyalose B, a Marine Macrolide Glycoside: Total Synthesis and Stereochemical Revision. *Strategies and Tactics in Organic Synthesis*. 2016; 12:143–168.
12. Zweifel T, Naubron J, Grützmacher H. Catalyzed Dehydrogenative Coupling of Primary Alcohols with Water, Methanol, or Amines. *Angew Chem Int Ed*. 2009; 48:559–563.
13. Trincado M, Grutzmacher H, Vizza F, Bianchini C. Domino Rhodium/Palladium-Catalyzed Dehydrogenation Reactions of Alcohols to Acids by Hydrogen Transfer to Inactivated Alkenes. *Chem Eur J*. 2010; 16:2751–2757. [PubMed: 20082396]
14. Annen S, Zweifel T, Ricatto F, Grutzmacher H. Catalytic Aerobic Dehydrogenative Coupling of Primary Alcohols and Water to Acids Promoted by a Rhodium(I) Amido N-Heterocyclic Carbene Complex. *ChemCatChem*. 2010; 2:1286–1295.
15. Balaraman E, Khaskin E, Leitus G, Milstein D. Catalytic Transformation of Alcohols to Carboxylic Acid Salts and H₂ Using Water as the Oxygen Atom Source. *Nature Chemistry*. 2013; 5:122–125.
16. Choi J, Heim LE, Ahrens M, Prechtel MHG. Selective Conversion of Alcohols in Water to Carboxylic Acids by in situ Generated Ruthenium Trans Dihydrido Carbonyl PNP Complexes. *Dalton Trans*. 2014; 43:17248–17254. [PubMed: 25019331]
17. Malineni J, Keul H, Möller M. A Green and Sustainable Phosphine-Free NHC-Ruthenium Catalyst for Selective Oxidation of Alcohols to Carboxylic Acids in Water. *Dalton Trans*. 2015; 44:17409–17414. [PubMed: 26390134] 17a Fujita K, Tamura R, Tanaka Y, Yoshida M, Onoda M, Yamaguchi R. Dehydrogenative Oxidation of Alcohols in Aqueous Media Catalyzed by a Water-Soluble Dicationic Iridium Complex Bearing a Functional N-Heterocyclic Carbene Ligand without Using Base. *ACS Catal*. 2017; 7:7226–7230.
18. Santilli C, Makarov IS, Fristrup P, Madsen RJ. Dehydrogenative Synthesis of Carboxylic Acids from Primary Alcohols and Hydroxide Catalyzed by a Ruthenium N-Heterocyclic Carbene Complex. *Org Chem*. 2016; 81:9931–9938.
19. Dai Z, Luo Q, Meng X, Li R, Zhang J, Peng T. Ru(II) Complexes Bearing 2,6-Bis(benzimidazole-2-yl)pyridine Ligands: a New Class of Catalysts for Efficient Dehydrogenation of Primary Alcohols to Carboxylic Acids and H₂ in the Alcohol/CsOH System. *J Organomet Chem*. 2017; 830:11–18.
20. Celaje JJA, Lu Z, Kedzie EA, Terrile NJ, Lo JN, Williams TJ. A Prolific Catalyst for Dehydrogenation of Neat Formic Acid. *Nature Com*. 2016; 7:11308.

21. Lu Z, Demianets I, Hamze R, Terrile NJ, Williams TJ. A Prolific Catalyst for Selective Conversion of Neat Glycerol to Lactic Acid. *ACS Catal.* 2016; 6:2014–2017.
22. This dimerization is known to be catalyzed by $[\text{IrCl}(\text{COD})]_2$ and $[\text{Cp}^*\text{IrCl}_2]_2$ in the presence of a strong base. See Matsu-ura T, Sakaguchi S, Obora Y, Ishii Y. Guerbet Reaction of Primary Alcohols Leading to β -Alkylated Dimer Alcohols Catalyzed by Iridium Complexes. *J Org Chem.* 2006; 71:8306–8308. [PubMed: 17025333]
23. Mako TL, Byers JA. Recent Advances in Iron-Catalysed Cross Coupling Reactions and Their Mechanistic Underpinning. *Inorg Chem Front.* 2016; 3:766–790.
24. Kawahara R, Fujita K, Yamaguchi R. N-Alkylation of Amines with Alcohols Catalyzed by a Water-Soluble Cp^* Iridium Complex: An Efficient Method for the Synthesis of Amines in Aqueous Media. *Adv Synth Catal.* 2011; 353:1161–1168. 24a Fujita K, Yamamoto K, Yamaguchi R. Oxidative Cyclization of Amino Alcohols Catalyzed by a Cp^*Ir Complex. Synthesis of Indoles, 1,2,3,4-Tetrahydroquinolines, and 2,3,4,5-Tetrahydro-1-benzazepine. *Org Lett.* 2002; 4:2691–2694. [PubMed: 12153211]
25. Berliner MA, Dubant SPA, Makowski T, Ng K, Sitter B, Wager C, Zhang Y. Use of an Iridium-Catalyzed Redox-Neutral Alcohol-Amine Coupling on Kilogram Scale for the Synthesis of a GlyT1 Inhibitor. *Org Process Res Dev.* 2011; 15:1052–1062.
26. Esteruelas MA, Oliván M, Oro LA, Schulz M, Sola E, Werner H. Synthesis, Molecular Structure and Reactivity of the Octahedral Iridium(III) Compound $[\text{IrH}(\eta^1, \eta^3\text{-C}_8\text{H}_{12})(\text{dppm})]$ [dppm = bis(diphenylphosphino)methane]. *Organometallics.* 1992; 11:3659–3664.
27. Olsen EPK, Madsen R. Iridium-Catalyzed Dehydrogenative Decarbonylation of Primary Alcohols with the Liberation of Syngas. *Chem Eur J.* 2012; 18:16023–16029. [PubMed: 23108889]
28. Olsen EPK, Singh T, Harris P, Andersson PG, Madsen R. Experimental and Theoretical Mechanistic Investigation of the Iridium-Catalyzed Dehydrogenative Decarbonylation of Primary Alcohols. *J Am Chem Soc.* 2015; 137:834–842. [PubMed: 25545272]
29. Melnick JG, Radosevich AT, Villagran D, Nocera DG. Decarbonylation of Ethanol to Methane, Carbon Monoxide and Hydrogen by a [PNP]Ir Complex. *Chem Commun.* 2010; 46:79–81.
30. Kloek SM, Heinekey DM, Goldberg KI. Stereoselective Decarbonylation of Methanol to Form a Stable Iridium(III) trans-Dihydride Complex. *Organometallics.* 2006; 25:3007–3011.
31. Cotton FA, Poli R. Ortho Metalation of Pyridine at a Diiridium Center. Synthesis and Spectroscopic and Crystallographic Characterization of NC_5H_4 - and $\text{N,N}'$ -Di-p-tolylformamidinato-Bridged Complexes of Diiridium(II). *Organometallics.* 1987; 6:1743–1751.
32. Takahashi Y, Nonogawa M, Fujita K, Yamaguchi R. C–H Activation on a Diphosphine and Hydrido-Bridged Diiridium Complex: Generation and Detection of an Active $\text{Ir}^{\text{II}}\text{--Ir}^{\text{II}}$ Species $[(\text{Cp}^*\text{Ir})_2(\mu\text{-dmpm})(\mu\text{-H})]^+$ *Dalton Trans.* 2008:3546–3552. [PubMed: 18594702]
33. Iali W, Green GGR, Hart SJ, Whitwood AC, Duckett SB. Iridium Cyclooctene Complex That Forms a Hyperpolarization Transfer Catalyst before Converting to a Binuclear C–H Bond Activation Product Responsible for Hydrogen Isotope Exchange. *Inorg Chem.* 2016; 55:11639–11643. [PubMed: 27934314]
34. Zell T, Milstein D. Hydrogenation and Dehydrogenation Iron Pincer Catalysts Capable of Metal-Ligand Cooperation by Aromatization/Deaomatization. *Acc Chem Res.* 2015; 48:1979–1994. [PubMed: 26079678]

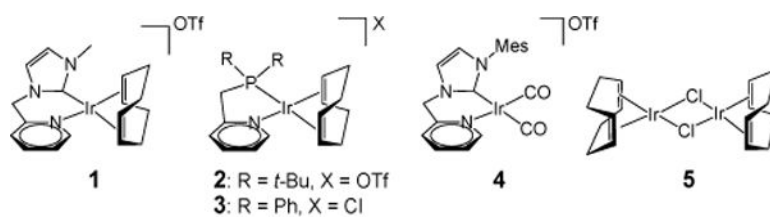


Figure 1.
Iridium Complexes 1-5.

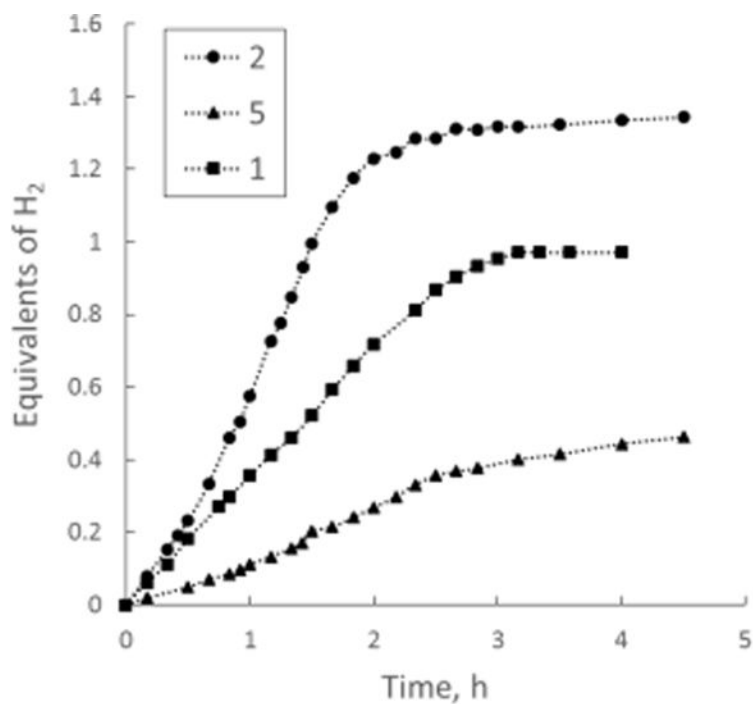


Figure 2. Hydrogen evolution profiles of **6f** dehydrogenation with **1**, **2**, and **5**. Conditions: a mixture of a catalyst (4×10^{-6} mol, 0.2 mol%), KOH (2.2 mmol), **6f** (2.0 mmol), and toluene (10 mL) was actively stirred at reflux (oil bath, 120 °C).

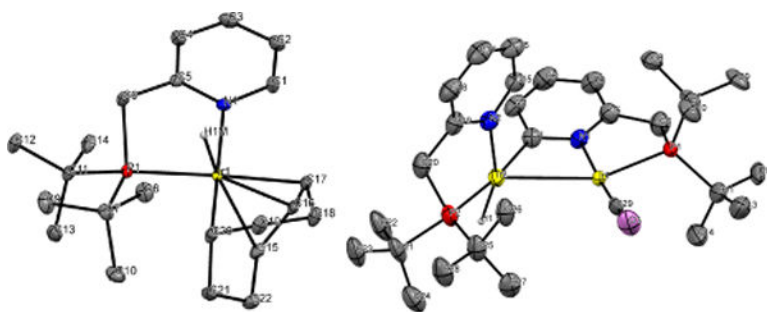


Figure 3. Molecular structures of **2b** (left) and **2c** (right) shown with 50% probability ellipsoids. Hydrogen atoms are omitted for clarity, except for localized hydrides.

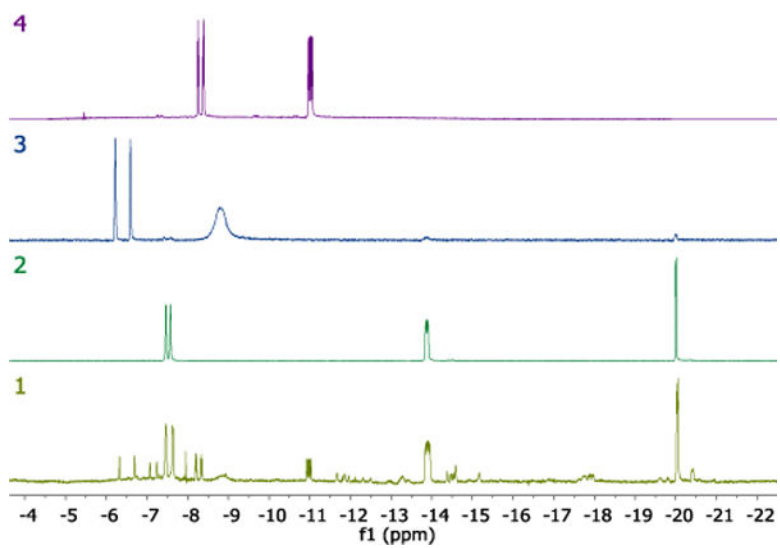
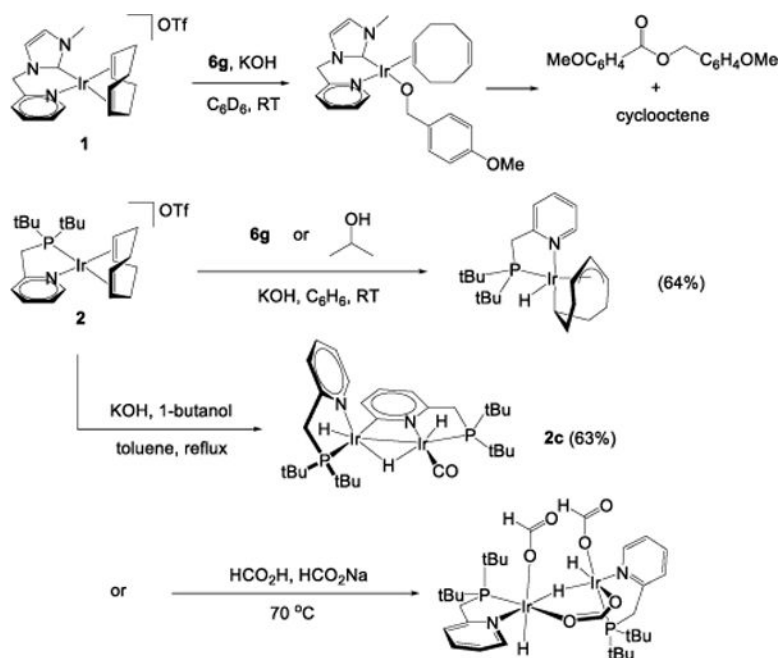
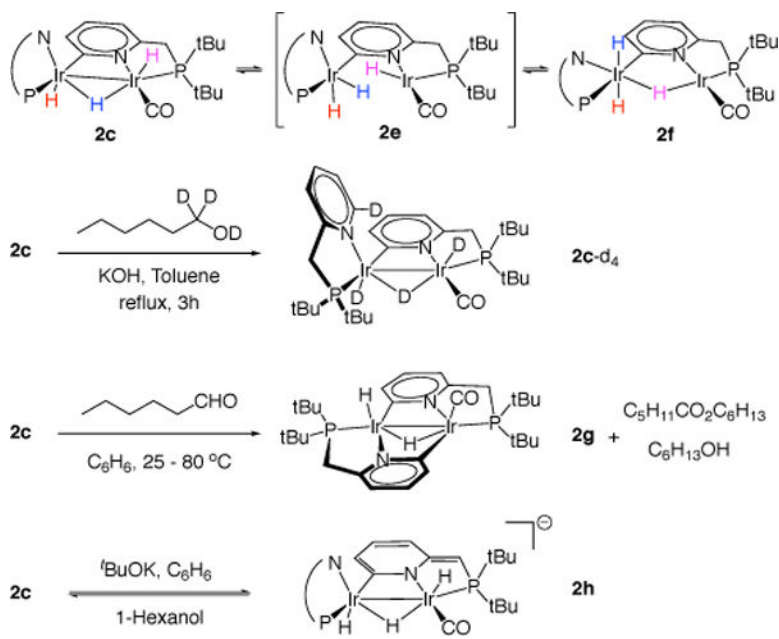


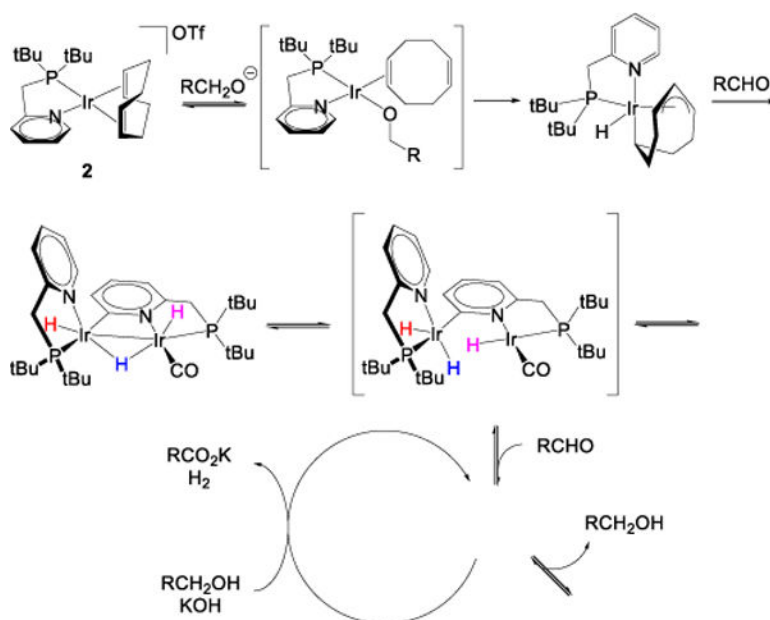
Figure 4. ^1H NMR spectra (600 MHz, C_6D_6) demonstrating IrH peaks: (1) mixture of complexes formed in the reaction between **2**, 1-butanol, and KOH in boiling toluene; (2) **2c**; (3) **2f**; (4) **2g**.



Scheme 1.
Reactions of Complexes **1** and **2**.



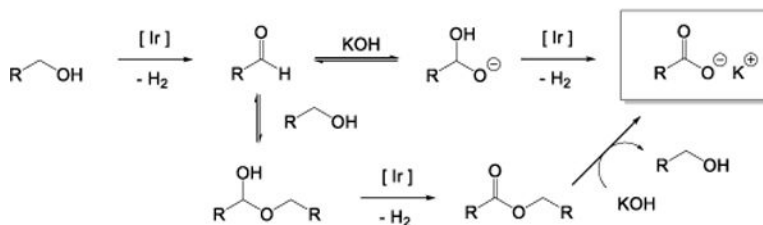
Scheme 2.
Reactions of Complex **2c**.

**Scheme 3.**

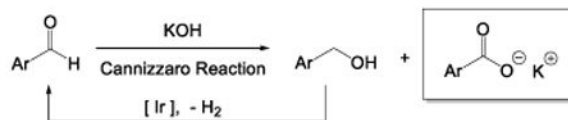
Mechanism of Pre-catalyst **2** Activation.^a

a. Colored labels on iridium hydride groups are not intended to imply specificity in hydride transfer steps, but simply to guide the reader. In fact, these hydrides equilibrate rapidly.

Tishchenko pathway cannot be excluded as a mechanism for carboxylate formation.

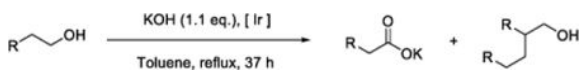


Oxidation of benzyl alcohols involves a Cannizzaro disproportionation.



Scheme 4.

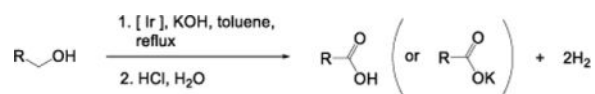
Mechanisms of Aldehyde and Carboxylate Formation.



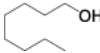
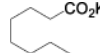

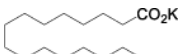
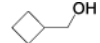
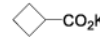
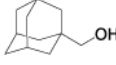
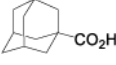
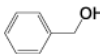
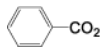
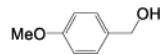
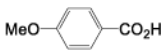
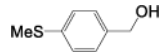
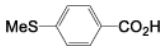
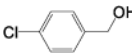
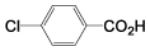
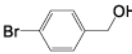
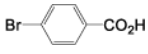
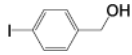
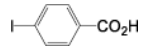
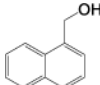
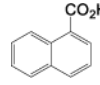
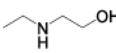
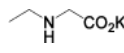
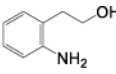
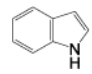
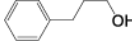
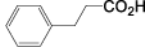
Table 1Selectivity Screening of Catalysts **1–5**.^a

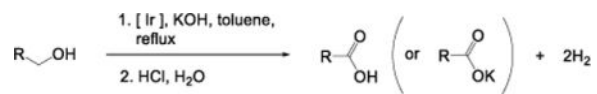
Entry	[Ir]	R	Carboxylate, %	Guerbet Alcohol, %
1	1	Ethyl	> 99	0
2	2	Ethyl	>99	0
3	1	n-Hexyl	99	1
4	2	n-Hexyl	95	5
5 ^b	1	n-Tetradecyl	90	10
6	2	n-Tetradecyl	92	8
7	3	n-Tetradecyl	77	23
8	4	n-Tetradecyl	77	23
9	5	n-Tetradecyl	76	24

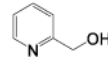
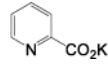
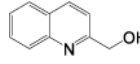
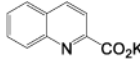
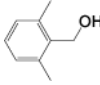
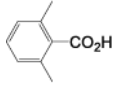
^aReaction conditions: a mixture of alcohol (2.1 mmol), KOH (2.4 mmol), catalyst (2.1×10^{-5} mol, 1 mol%), and toluene (4 mL) was stirred at reflux for 37 h (oil bath, 120 °C). The yields were derived from ¹H NMR spectra.

^b0.1 mol% of **1** was used.

Table 2Substrate Scope for Dehydrogenation of Primary Alcohols Using Pre-Catalysts 1 and 2.^a

Entry	Alcohol	Product	Catalyst Time (h) Isolated yield (%)
1			1 (0.2%) 40 96
2			1 (0.2%) 40 90
3			1 (0.2%) 40 85
4			2 (0.2%) 40 81
5			2 (0.4%) 75 77
6			2 (0.2%) 40 98
7			1 (0.4%) 36 79
8			1 (0.1%) 40 74
9			2 (0.1%) 20 80
10			1 (0.1%) 15 40
11			2 (0.3%) 18 42
12			2 (0.2%) 40 84
13			2 (0.2%) 40 82
14			2 (0.2%) 13 80
15			2 (0.2%) 40 80



Entry	Alcohol	Product	Catalyst Time (h)	Isolated yield (%)
16			1	(0.2%) 20 63
17			2	(0.2%) 40 65
18			1	(0.1%) 15 0

^aReaction conditions: a mixture of an alcohol (2.0 mmol), KOH (2.2 mmol), catalyst, and toluene (10 mL) was stirred at reflux.